AD-A052 908 DENVER UNIV COLO DEPT OF MATHEMATICS F/G 20/1
A SURVEY OF RECENT PROGRESS ON INVERSE PROBLEMS.(U)
DEC 77 N BLEISTEIN, J K COHEN N00014-76-C-0079
UNCLASSIFIED MS-R-7806 NL

END
DATE FILMED
5-78
DDC

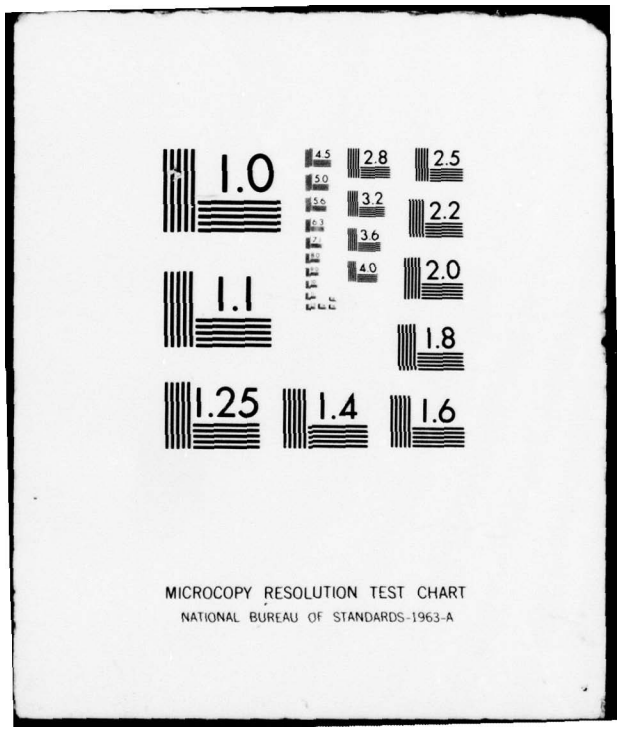
1.0
1.1
1.25
1.4
1.6
1.8
2.0
2.2
2.5
2.8
3.2
3.6
4.0
4.5
5.0
5.6
6.3
7.1
MICROCOPY RESOLUTION TEST CHART
NATIONAL BUREAU OF STANDARDS-1963-A

MS-R-7806

12
B 5

A SURVEY OF RECENT PROGRESS ON INVERSE PROBLEMS

by

Norman Bleistein and Jack K. Cohen

Department of Mathematics
University of Denver
Colorado Seminary

The preparation of this report was supported by the Office of Naval Research.

MS-R-7806

A SURVEY OF RECENT PROGRESS ON INVERSE PROBLEMS

by

Norman Bleistein and Jack K. Cohen

Department of Mathematics
University of Denver
Colorado Seminary

The preparation of this report was supported by the Office of Naval Research.

TABLE OF CONTENTS

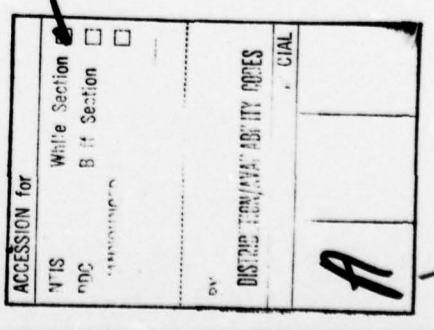

Introduction

Over the past few years, the authors have been engaged in a coordinated research program on inverse problems. By this time, the results have been spread over a number of different papers. Thus, it is the considered opinion of the authors that a review of the present state of this research be written. This review also provides an opportunity to filter some of the work that has proven to be of less interest and to incorporate into the presentation new insights that have been developed during this research project.

This report describes the three main segments in this research program:

(i) physical optics far field inverse scattering (denoted by the acronym, POFFIS);

(ii) seismic or subsurface profiling in media with small variations in propagation speed;

(iii) analysis of the inverse source problem.

1. The POFFIS Identity

The POFFIS identity was originally derived by BOJARSKI [1]. Analysis of the basic identity and its extensions can be found in LEWIS [2], BOJARSKI [3], PERRY [4], TABBARA [5,6], ROSENBAUM-RAZ [7], BLEISTEIN [8,9] and MAGER and BLEISTEIN [10]. The problem of interest here is reconstruction of the image of a convex scatterer from observations of the high frequency far field scattering from the object in response to a known probing signal.

The POFFIS identity relates the scattered field to the Fourier transform of the characteristic function of the scatterer. The characteristic function is equal to unity in the region occupied by the scatterer and zero elsewhere. Thus, knowledge of this function makes possible the reconstruction of an image of the scatterer. The Fourier transform of the characteristic function is itself a function of a vector transform variable, $\underline{k}$. The magnitude of the vector is proportional to frequency; the direction of the vector is determined by the source-receiver directions. Consequently, in any practical situation, with limited bandwidth and directions of observation, the Fourier transform is known only in some aperture limited--band limited and aspect angle limited--domain in $\underline{k}$ space. The problem of extracting information about the characteristic function from a high frequency aperture limited Fourier transform is solely a question in the Fourier analysis of piecewise constant (in this case zero-one) functions. The problem is discussed from this point of view in Section 1.3 and will prove useful in the discussions in Sections 2.1--2.3 below.

1.1 Derivation of the POFFIS Identity

A point source located at $\underline{x}_0$ in Figure 1, gives rise to a signal, $u_I(\underline{x}, \underline{x}_0, \omega)$, which is a solution of the reduced wave equation,

$$(1.1) \qquad \nabla^2 u_I + \omega^2 u_I/c^2 = -\delta(\underline{x} - \underline{x}_0); \quad \underline{x} = (x_1, x_2, x_3).$$

Here, ∇^2 is the three-dimensional Laplacian, $\delta(\underline{x})$ is a three-dimensional Dirac delta function and

$$(1.2) \qquad u_I(\underline{x}, \underline{x}_0, \omega) = \exp\{i\omega|\underline{x} - \underline{x}_0|/c\} / (4\pi|\underline{x} - \underline{x}_0|).$$

The signal u_I is incident upon a convex scatterer (B in Figure 1), giving rise to a scattered signal u_S. The scattered field has the following integral representation in terms of its values on ∂ B, the boundary of B (See, for example, BAKER and COPSON [11]):

$$(1.3) \qquad u_S(\underline{x}, \underline{x}_0, \omega) = \int_{\partial B} \left\{ u_S(\underline{x}', \underline{x}_0, \omega) \frac{\partial g}{\partial n}(\underline{x}, \underline{x}', \omega) \right.$$

$$\left. - g(\underline{x}, \underline{x}', \omega) \frac{\partial u_S}{\partial n}(\underline{x}', \underline{x}_0, \omega) \right\} dA.$$

Here the integral is over the scattering surface in prime variables, g is the Green's function, given by (1.2) with $\underline{x}_0$ replaced by $\underline{x}'$, and $\partial/\partial n$ denotes the outward normal derivative to ∂B.

At this point, the *physical optics* approximations are introduced (See [11]). To do so, attention is first restricted to the backscatter case, $\underline{x} = \underline{x}_0$ in (1.3).† Then, it is assumed that $\underline{x}_0$ is very far from the scatterer. Thus, in a coordinate system with origin "near" or inside the scatterer, $x_0 = |\underline{x}_0| >> 1$. The scatterer is now divided into two parts, a lit side $L(\hat{x}_0)$ and a dark side $D(\hat{x}_0)$ with respect to "physical optics" illumination by a plane wave from the direction of $\underline{x}_0$, that direction denoted by the unit vector $\hat{x}_0$ as shown in Figure 1.

Under the assumption that the scatterer is acoustically hard (so that the exact boundary condition is that the normal derivative of the total field is zero on ∂B) the physical optics approximations are as follows.

$$(1.4) \qquad u_S = \frac{\partial u_S}{\partial n} = 0 \qquad \underline{x}' \text{ on } D(\hat{x}_0) \ ;$$

$$(1.5) \qquad u_S = u_I, \quad \frac{\partial u_S}{\partial n} = -\frac{\partial u_I}{\partial n}, \quad \underline{x}' \text{ on } L(\hat{x}_0).$$

For the acoustically soft case (where the exact boundary condition is that the total field is zero on ∂B), the minus sign in the second equation in (1.5) is deleted and a minus sign is inserted on the right side of the first equation in (1.5). This will only result in an overall minus sign in the results to be derived and, hence, only the case (1.4,5) will be discussed below.

---

† The physical optics approximations remain valid for "small" separation angle between $\underline{x}$ and $\underline{x}_0$.

Applying all of these results to (1.3) yields

$$(1.6) \qquad u_S(\underline{x}_0, \underline{x}_0, \omega) = \int_{L(\hat{x}_0)} \left\{ \frac{\partial}{\partial n} \left\{ u_I^2(\underline{x}', \underline{x}_0, \omega) \right\} \right\} dA.$$

The far field assumption is now made, namely that

$$(1.7) \qquad x_0 >> x, \quad x = |\underline{x}|, \quad x \text{ on } \partial B.$$

Then, for $\underline{x}$ on ∂B, $|\underline{x} - \underline{x}_0|$ may be expanded as follows:

$$(1.8) \qquad |\underline{x} - \underline{x}_0| = x_0 - \underline{x} \cdot \hat{x}_0 + O(x^2 / x_0).$$

The result (1.2) is now inserted in (1.6) and then from (1.8), a two-term expansion is used in the phase and a one-term expansion is used in the amplitude to yield

$$(1.9) \qquad u_S(\underline{x}, \underline{x}_0, \omega) = \frac{\exp\{2i\omega x_0/c\}\, \rho(\omega \hat{x}_0/c)}{(4\pi x_0)^2}.$$

Here $\rho(\omega \hat{x}_0/c)$ is a *phase and range normalized far field scattering amplitude* given by

$$(1.10) \qquad \rho(\omega \hat{x}_0/c) = \int_{L(\hat{x}_0)} \left\{ \frac{\partial}{\partial n} \left\{ \exp\{-2i\omega \underline{x}' \cdot \hat{x}_0/c\} \right\} \right\} dA.$$

If a similar experiment is performed from the opposite direction, the result is

$$(1.11)\qquad \rho(-\omega\,\hat{x}_0/c) = \int_{D(\hat{x}_0)} \left\{ \frac{\partial}{\partial n} \left\{ \exp\{2i\omega\,\underline{x}'\cdot\hat{x}_0/c\} \right\} \right\} dA.$$

From (1.10) and (1.11), it follows that

$$(1.12)\qquad \rho(\omega\,\hat{x}_0/c) + \rho^*(-\omega\,\hat{x}_0/c) = \int_{\partial B} \frac{\partial}{\partial n} \left\{ \exp\{-2i\omega\,\underline{x}'\cdot\hat{x}_0/c\} \right\} dA.$$

Here $(^*)$ denotes complex conjugate.

Applying the divergence theorem here yields

$$(1.13)\qquad \rho(\omega\,\hat{x}_0/c) + \rho^*(-\omega\,\hat{x}_0/c) = \int_B \nabla^2 \left\{ \exp\{-2i\omega\,\underline{x}'\cdot\hat{x}_0/c\} \right\} dV$$

$$= -(4\omega^2/c^2)\ \tilde{\gamma}(2\omega\,\hat{x}_0/c).$$

Here,

$$(1.14) \qquad \tilde{\gamma}(\underline{k}) = \int_B \exp\{-i\underline{k} \cdot \underline{x}'\}\, dV, \quad \underline{k} = (k_1, k_2, k_3).$$

The function $\tilde{\gamma}(\underline{k})$ is the Fourier transform of the function

$$(1.15) \qquad \gamma(\underline{x}) = \begin{cases} 1, & \underline{x} \text{ in } B \\ 0 & \underline{x} \text{ not in } B \end{cases}.$$

This function is the characteristic function of the region B. If $\gamma(\underline{x})$ is known, the region B is known. (Actually, if the discontinuity of $\gamma(\underline{x})$ is known, B is known.) The result (1.13) relates the Fourier transform of $\gamma(\underline{x})$ to the phase and range normalized scattering amplitude. The value of the transform variable is

$$(1.16) \qquad \underline{k} = 2\omega \hat{x}_0/c.$$

Thus, (1.13) is the POFFIS identity.

It should be noted that the POFFIS identity is a result derived for high frequency only. Thus, the identity is suspect when used to determined $\tilde{\gamma}(\underline{k})$ for small values of $|\underline{k}|$. Often, as a practical matter, low frequency (and hence, small $|\underline{k}|$) information is simply not available. Furthermore, the obstacle often cannot be probed from all directions $\hat{x}_0$. Thus, one is faced with the limited aperture problem mentioned in the introduction and addressed in Section 1.3.

1.2 The POFFIS Identity for One-Sided Viewing of Anomalies in a Geological Structure

In geophysical or oceanographic exploration, one is faced with the problem of mapping a reflector from one-sided backscatter information, only. As an example of this type, Figure 2 depicts an anticlinal perturbation B of finite extent in a plane R. The surface to be detected here is S which is the same as R except on the anticline.

With u_S denoting the field scattered by S, and making the same approximations as in the previous section, (1.6) is replaced by

$$(1.17) \qquad u_S(\underline{x}_0, \underline{x}_0, \omega) = \int_S \frac{\partial}{\partial n} \left\{ u_I{}^2(\underline{x}_0, \underline{x}', \omega) \right\} dA.$$

In the absence of the anticline, the backscattered field, denoted by u_R, has the *exact* representation

$$(1.18) \qquad u_R(\underline{x}_0, \underline{x}_0, \omega) = \int_R \frac{\partial}{\partial n} \left\{ u_I{}^2(\underline{x}_0, \underline{x}', \omega) \right\} dA.$$

Thus, the difference between the two fields u_S and u_R is given by

$$(1.19) \qquad u_S - u_R = \int_{\partial B} \frac{\partial}{\partial n} \left\{ u_I{}^2(\underline{x}_0, \underline{x}', \omega) \right\} dA.$$

Proceeding now as in the previous section leads to the result

$$(1.20) \qquad u_S - u_R = \frac{\exp\{2i\omega\, x_0/c\}\ \ \rho(\omega \hat{x}_0/c)}{(4\pi x_0)^2} \ ,$$

with ρ now given by

$$(1.21) \qquad \rho(\omega\, \hat{x}_0/c) = \int_{\partial B} \frac{\partial}{\partial n} \exp\{-\, 2i\omega \underline{x}' \cdot \hat{x}_0/c\}\ dA$$

$$= -(4\omega^2/c^2)\ \tilde{\gamma}\ (2\omega \hat{x}_0/c) \ .$$

Here, $\tilde{\gamma}\ (\underline{k})$ is again the Fourier transform given by (1.14, 15) but with B defined by Figure 2.

In (1.20), u_S is observed for $\hat{x}_0$ having a positive first component. The function u_R does <u>not</u> have to be observed since it is a mathematical construct defined by (1.18). Thus, $\tilde{\gamma}(\underline{k})$ is known only in the upper half $\underline{k}$ space and this POFFIS identity does not suffice to generate B. To overcome this difficulty the region B^* of Figure 3 is introduced. This region is generated by projecting B through the origin. That is, if $\underline{x}$ is in B, then $-\underline{x}$ is in B^*.

The characteristic function of the region $B + B^*$ is denoted by $\psi(\underline{x})$. Thus,

$$(1.22) \qquad \psi(\underline{x}) = \begin{cases} \gamma(\underline{x}) & x, \geq 0 \\ \gamma(-\underline{x}) & x, < 0 \end{cases} \ .$$

Its Fourier transform is given by

$$(1.23) \qquad \tilde{\psi}(\underline{k}) = \int_{B + B^*} \exp\{i\underline{k} \cdot \underline{x}\} dV = 2 \int_{B} \cos(\underline{k} \cdot \underline{x})\, dV,$$

or, using (1.14)

$$(1.24) \qquad \tilde{\psi}(\underline{k}) = 2\ \mathrm{Re}\ \tilde{\gamma}(\underline{k}).$$

Therefore, $\tilde{\gamma}(\underline{k})$ is determined by taking twice the real part of $\tilde{\gamma}(\underline{k})$ for $\underline{k}$ in the upper half-space and by extending this function as an even function of $\underline{k}$ to obtain its value in the lower half-space. By inverting, one then finds that

$$(1.25) \qquad \gamma(\underline{x}) = \frac{1}{2\pi^3} \int_{k_1 \geq 0} \mathrm{Re}\ \tilde{\gamma}(\underline{k}) \cos(\underline{k} \cdot \underline{x}) d^3k, \quad x_1 \geq 0.$$

In this case, then (1.20, 21, 25) constitute the POFFIS identity.

For a synclinal structure (with B a region below R), the result (1.19) is replaced by its negative. This change in sign persists throughout and the syncline is then revealed by the processing in (1.25) yielding a function equal to -1 or zero for $x_1 \geq 0$.

For a cylindrical anomaly, such as the anticline in Figure 4, the analysis must be modified. Firstly, the medium is

probed only alone a line parallel to the x_2 axis, say with $x_3 = 0$. Then in (1.17) and (1.18), x_{30} is set equal to zero and the integration in x'_3 is carried out by the method of stationary phase [12]. The result is

$$(1.26) \qquad u_S - u_R = \frac{\exp\{2i\omega x_0/c + i\pi/4\}}{4(2\pi x_0)^{3/2}} \rho(2\omega \hat{x}_0/c) \ .$$

Here,

$$(1.27) \qquad \rho(\underline{\kappa}) = \kappa^{3/2} \int_{\Sigma} \exp\{-i\underline{\kappa} \cdot \underline{x}'\} \, dA; \ \underline{\kappa} = (k_1, k_2, 0)$$

and Σ is the cross-sectional area of B in the (x_1, x_2) plane. Because B is a cylinder, when Σ is known, B is known.

For the region Σ, its characteristic function $\sigma(x_1, x_2)$ is defined by

$$(1.28) \qquad \sigma(x_1, x_2) = \begin{cases} 1, & (x_1, x_2) \text{ in } \Sigma \\ 0 & (x_1, x_2) \text{ not in } \Sigma \end{cases} .$$

It then follows from (1.27) that

$$(1.29) \qquad \tilde{\sigma}(\underline{\kappa}) = \kappa^{-3/2} \tilde{\rho}(\underline{\kappa}).$$

By using the same symmetry arguments as above, one finds that

$$(1.30) \qquad \sigma(x_1, x_2) = \frac{1}{\pi^2} \int_{\kappa_1 \geq 0} \mathrm{Re}\ \tilde{\sigma}(\underline{\kappa})\ \cos(\underline{\kappa} \cdot \underline{x})\ d^2\kappa,\ x_1 \geq 0.$$

1.3 An Approach to the Limited Aperture Problem for the POFFIS Identity

As noted in earlier sections, complete information required for Fourier inversion of the POFFIS identity is not available in practice. That high frequency far field scattering data should suffice to reconstruct the image of the scatterer has been rigorously proven by MAJDA [13].

In this section a method for processing both band limited and aspect angle limited data will be described. The method was originally proposed by BOJARSKI [3] for high frequency band limited data and further analyzed for this case in [9]. Limited aspect angle is discussed in [10].

The method is based solely on the features of the Fourier transform of piecewise constant (in this case, one-zero) functions. The only additional assumption made here is that the region in which the function equals unity is convex, finite and has a smooth boundary surface. These are exactly the assumptions made for the scatterer B of Section 1.1. Indeed, the function to be analyzed here is $\gamma(\underline{x})$ defined by (1.15) and its Fourier transform $\tilde{\gamma}(\underline{k})$ defined by (1.14).

The approach to be presented here is based on the following ideas from one-dimensional Fourier analysis. If $\gamma(x)$ is a one-dimensional characteristic function, then its first derivative consists of two Dirac delta functions at the boundaries of the

region where $\gamma(x) = 1$. The function $\delta(x-a)$ has Fourier transform $\exp\{-ika\}$ and band limited inverse transform

$$(1.31) \qquad \delta(x-a) \simeq \pi^{-1}(x-a)^{-1} \sin[k(x-a)] \Big|_{k_-}^{k_+} ,$$

with $k_{\pm}$ the band limits. This function peaks at $x = a$, with peak value $(k_+ - k_-)/\pi$. Thus, the boundaries of the region of interest are readily recognized from this band limited processing. The purpose of this section is to show that this is true in two- and three-dimensions, as well, and also to show the effects of aspect angle limitations in these cases.

For the function $\gamma(\underline{x})$ defined by (1.15), the directional derivative is the direction defined by the unit vector $\hat{p}$ is given by

$$(1.32) \qquad \Delta(\underline{x}, \hat{p}) = -\hat{p} \cdot \nabla\gamma(\underline{x}).$$

If ∂B is defined by $\Phi(\underline{x}) = 0$, with Φ negative in B and positive outside of B, then

$$(1.33) \qquad \Delta(\underline{x}, \hat{p}) = \hat{p} \cdot \nabla\Phi\delta(\Phi).$$

The Fourier transform of Δ is

$$(1.34) \qquad \tilde{\Delta}(\underline{k}, \hat{p}) = \int \hat{p} \cdot \nabla\Phi(\underline{\xi})\delta\left[\Phi(\underline{\xi})\right] \exp\{-i\underline{k} \cdot \underline{\xi}\}\, dV.$$

Here the domain of integration is all of $\underline{\xi}$-space. The integration normal to the boundary is readily calculated by exploiting the properties of the delta function. The result is

$$(1.35) \qquad \tilde{\Delta}(\underline{k}, \hat{p}) = \int_{\partial B} \hat{p} \cdot \hat{n} \exp\{-i\underline{k} \cdot \underline{\xi}\} \, dA.$$

Here $\hat{n}$ is the outward unit normal to ∂B.

The aperture limited inverse transform of $\tilde{\Delta}$ will be denoted by Δ_1. If $A_p(\underline{k})$ denotes the aperture in $\underline{k}$ space, then

$$(1.36) \qquad \Delta_1(\underline{x}, \hat{p}) = \frac{1}{(2\pi)^3} \int_{A_p(\underline{k})} d^3k \int_{\partial B} dA \, \hat{p} \cdot \hat{n} \exp\{i\underline{k} \cdot (\underline{x} - \underline{\xi})\}.$$

The apertures of interest are those for which $k = |\underline{k}|$ ranges between two values k_- and k_+ and the angle of $\underline{k}$ is restricted to some region Ω. Thus,

$$(1.37) \qquad \Delta_1(\underline{x}, \hat{p}) = \frac{1}{(2\pi)^3} \int_{k_-}^{k_+} k^2 dk \int_{\Omega} d\Omega \int_{\partial B} dA \, \hat{p} \cdot \hat{n} \exp\{i\underline{k} \cdot (\underline{x} - \underline{\xi})\}.$$

Here $d\Omega$ is the solid angle element in $\underline{k}$ space.

The four fold integral over Ω and ∂B can be calculated by the method of four-dimensional stationary phase [12]. The integration over k can then be done explicitly. The method is described in [10], but

the form of the result presented here is due to Armstrong [14]. The conditions that the phase be stationary are as follows. Firstly, the point $\underline{\xi}$ on ∂B must be such that $\underline{x} - \underline{\xi}$ is perpendicular to ∂B. Secondly, the angles of $\underline{k}$ are such that $\underline{x} - \underline{\xi}$ and $\underline{k}$ are colinear or anticolinear. Thus, the stationary points in $\underline{\xi}$ and $\underline{k}$ are such that $\underline{x} - \underline{\xi}$ and $\underline{k}$ lie along the normal to ∂B at the stationary point.

For each choice of $\underline{x}$ there may be one or more stationary points (or none at all!). If the contribution from each stationary point is denoted by $\Delta_2(\underline{x}, \hat{p})$, then one finds that asymptotically

$$(1.38) \qquad \Delta_2(\underline{x}, \hat{p}) = (2\pi)^{-1} \hat{n}\cdot\hat{p} \; (1 - \mu K_1 D)^{-\frac{1}{2}}(1 - \mu K_2 D)^{-\frac{1}{2}} \cdot D^{-1} \left\{ \sin(kD) - i[\cos(kD) - 1] \right\} \Big|_{k = k_-}^{k_+} .$$

Here,

$$(1.39) \qquad D = |\underline{x} - \underline{\xi}| \; ;$$

K_1 and K_2 are the principal curvatures of ∂B at the stationary point; $\mu = +1$ or -1 according to whether $\underline{x} - \underline{\xi}$ and $\hat{n}$ are anticolinear or colinear at the stationary point.

The real part Δ_2 is seen to have the same qualitative behavior for D small as the one-dimensional result (1.31). Furthermore,

$$(1.40) \qquad \lim_{D \to 0} \Delta_2(\underline{x}, \hat{p}) = (2\pi)^{-1} \hat{n}\cdot\hat{p} \quad (k_+ - k_-).$$

For each point on ∂B the contributions from stationary points with $D = 0$ will dominate all other contributions to $\Delta_1(\underline{x}, \hat{p})$ if the bandwidth is sufficiently broad. There can be at most two such contributions. This will occur if the region Ω contains both the vectors $\hat{k} = \hat{n}$ and $\hat{k} = -\hat{n}$ for the given stationary point, $\underline{\xi}$.

In [9], the following test of this method, as applied to the POFFIS identity, was carried out. The exact backscatter solution for a sphere of unit radius was used to generate $\rho(\omega\hat{x}_0/c)$ for the POFFIS identity (1.13). The angular aperture Ω was taken to be unrestricted; i.e., all angles were used. The vector $\hat{p} = (1, 0, 0)$ was used and $\Delta_1(\underline{x}, \hat{p})$ was calculated for $x_2 = x_3 = 0$. The angular integrations were carried out numerically and the integration in k was done numerically with the trapezoid rule. An example of the output of this processing is shown in Figure 5. The circles represent the theoretical results based on the asymptotic analysis presented here. In this case, $k_- = 15.75 \simeq 5\pi$, $k_+ = 31.5 \simeq 10\pi$. At the peak, the percentage error between theory and computation was .3%.

The two-dimensional analog of the results presented here is carried out in exactly the same manner. In (1.37), ∂B would now be a curve and $d\Omega$ is replaced by $d\theta$, the polar angle of $\underline{k} = (k_1, k_2)$. The factor $(2\pi)^{-3}$ is replaced by $(2\pi)^{-2}$. The result (1.38) is now replaced by

$$(1.41)\qquad \Delta^2(\underline{x}, \hat{p}) = (2\pi)^{-1}\, \hat{n}\cdot\hat{p}\;\; (1 - \mu KD)^{-\frac{1}{2}}$$

$$\cdot\, D^{-1}\left\{ \sin(kD) - i[\cos(kD) - 1] \right\} \Bigg|_{k_-}^{k_+} .$$

Here μ and D are as defined below (1.38).

In [15], the two-dimensional result was tested for an ellipse with semi-axes of length one and two. The result for full angular aperture k range 9 to 27 and $\hat{p} = (1, 0)$ is shown in Figure 6. The third dimension (the value of Δ_2) is laid back down in the plane. On each line the height is normalized with respect to maximum height. Furthermore, the maximum on each line is tested against the absolute maximum. When this relative maximum falls below a critical value, the entire line is zeroed out. This insures, for example, that "noise" will not be enhanced outside of the vertical extent of the ellipse. Nonetheless, near the top and bottom of the ellipse, where $\hat{p} \cdot \hat{n}$ is nearly zero, there is clearly some loss in resolution. This region could be resolved better if $\hat{p}$ were chosen to be (0, 1).

In Figure 7, limited aperture process is shown for Ω consisting of two quadrants. There is some "spill-over" outside of the angular aperture, but, for the most part the ellipse is reproduced as in the previous diagram, but only for the region for which the normals to the ellipse lie in the angular aperture in $\underline{k}$ space.

In [10], further examples are carried out in which numerical data is generated for backscattering by a circular cylinder. The results confirm the POFFIS method of Section 1 as well as the Fourier analysis of this section.

It should be noted that near the evolute of ∂B, (1.38) or (1.41) becomes invalid. In [14], ARMSTRONG shows that the contribution from that region is extremely small relative to the peak value of Δ_2 at $D = 0$.

1.4 POFFIS in the Time Domain

Returning to (1.9), the inverse time transforms of u_S and ρ are defined to be U_S and V, respectively. From (1.9) it follows that

$$(1.42) \qquad V(\hat{x}_0, t) = (4\pi x_0)^2 U_S(\underline{x}_0, t + 2x_0/c).$$

That is, the Fourier transform of the phase and range normalized scattering amplitude is a range normalized and time-delayed scattering amplitude in the time domain and thus, is as easily observable as $\rho(\omega\hat{x}_0/c)$. The objective of this section is to show how to use this result and the basic POFFIS identity to derive a POFFIS identity in the time domain.

The Fourier inversion in (1.13) is first expressed as an integral in polar coordinates. The result is

$$(1.43) \qquad \gamma(\underline{x}) = -\frac{1}{4\pi^3 c} \int_0^\infty d\omega \int_\Omega d\Omega \{\rho(\omega\hat{x}_0/c) + \rho^*(-\omega\hat{x}_0/c)\}$$

$$\cdot \exp\{2i\omega\hat{x}_0 \cdot \underline{x}/c\} \quad .$$

Here, Ω denotes the unit sphere with variable $\hat{x}_0$ and differential solid angle element on it, $d\Omega$. The volume element in polar coordinates has a factor of ω^2; however, the integrand also has a

factor ω^{-2} arising from solving for $\tilde{\gamma}$.

This result may be rewritten as an integral over the hemisphere centered at $\hat{x}_0$. The result is

$$(1.44)\qquad \gamma(\underline{x}) = -\frac{1}{4\pi^3 c}\int_0^\infty d\omega \int_{\Omega/2} d\Omega \left\{ [\rho(\omega\hat{x}_0/c) + \rho^*(-\omega\hat{x}_0/c)] \cdot \exp\{2i\omega\hat{x}_0 \cdot \underline{x}/c\} + [\rho(-\omega\hat{x}_0/c) + \rho^*(\omega\hat{x}_0/c)] \cdot \exp\{-2i\omega\hat{x}_0 \cdot \underline{x}/c\} \right\} .$$

Here, the second pair of terms, with $\hat{x}_0$ replaced by $-\hat{x}_0$, provides the integral over the back hemisphere. From the definitions of ρ in (1.10, 11), it should be recalled that these terms are calculated by integrating over regions $L(-\hat{x}_0)$ and $D(-\hat{x}_0)$, respectively. These, in turn are just $D(\hat{x}_0)$ and $L(\hat{x}_0)$ respectively. Furthermore, from (1.11),

$$(1.45)\qquad \rho^*(\omega\hat{x}_0/c) = \rho(-\omega\hat{x}_0/c),$$

where now, the change of sign is in ω, with $\hat{x}_0$ and hence $L(\hat{x}_0)$ remaining unchanged. Thus, the fourth term provides the extension of the first term to negative frequencies; the second term provides the same extension of the third term. Thus,

$$(1.46)\qquad \gamma(\underline{x}) = -\frac{1}{4\pi^3 c}\int_{-\infty}^{\infty} d\omega \int_{\Omega/2} d\Omega \Big\{ \rho(\omega \hat{x}_0/c)\, \exp\{2i\omega \hat{x}_0 \cdot \underline{x}/c\} + \rho(-\omega \hat{x}_0/c)\, \exp\{-2i\omega \hat{x}_0 \cdot \underline{x}/c\} \Big\} .$$

Here, ρ in the first line is defined by (1.10) and in the second line by (1.11). However, again using the fact that $D(\hat{x}_0) = L(-\hat{x}_0)$, the result can again be written as an integral over a sphere:

$$(1.47)\qquad \gamma(\underline{x}) = -\frac{1}{4\pi^3 c}\int_{-\infty}^{\infty} d\omega \int_{\Omega} d\Omega\ \rho(\omega \hat{x}_0/c)\, \exp\{2i\omega \hat{x}_0 \cdot \underline{x}/c\} .$$

The inverse time transform of ρ was defined to be V. Therefore, (1.47) can be rewritten as

$$(1.48)\qquad \gamma(\underline{x}) = -\frac{1}{4\pi^3 c}\int_{\Omega} d\Omega\ V(\hat{x}_0, -2\hat{x}_0 \cdot x/c) .$$

This is the POFFIS identity in the time domain.

The result (1.47) also provides an alternative to the POFFIS identity (1.13). In the form (1.46), the requirement of combining "front side" and "back side" observations before Fourier synthesis has been dispensed with. There is still a double covering in $\underline{k}$ space in (1.47), but this may be overcome by using (1.44) to conclude that

$$(1.49)\qquad \gamma(\underline{x}) = -\frac{Re}{2\pi^3 c}\int_0^\infty d\omega \int_\Omega d\Omega\ \rho(\omega\hat{x}_0/c)\exp\{2i\omega\hat{x}_0\cdot\underline{x}/c\}\ .$$

In this form, the integral is again a Fourier transform. When (1.9) is used and the integral is expressed again in terms of

$$(1.50)\qquad \underline{k} = \omega\hat{x}_0/c\ ,\qquad \hat{k} = \hat{x}_0\ ,$$

the result becomes

$$(1.51)\qquad \gamma(\underline{x}) = -8\pi^{-1}\,\mathrm{Re}\int k^{-2}d^3k\ x_0^2 u_S(\hat{kx}_0,\ \hat{kx}_0,\ ck)\cdot\exp\{2i\underline{k}\cdot\underline{x} - 2ikx_0\}\ .$$

Similarly, one can show that for $j = 1, 2, 3$,

$$(1.52)\qquad \frac{\partial\gamma(\underline{x})}{\partial x_j} = 16\pi^{-1}\,\mathrm{Im}\int k_j k^{-2}d^3k\ x_0^2 u_S(\hat{kx}_0,\ \hat{kx}_0,\ ck)\cdot\exp\{2i\underline{k}\cdot\underline{x} - 2ikx_0\}\ .$$

In these two equations x_0 may be a function of $\hat{x}_0$ (i.e., the observation distance may be different in different directions). Thus, in general, x_0 must remain under the integral sign.

2. An Inverse Method for Determining Small Inhomogeneities In a Medium

When a medium is known to have small and perhaps slowly varying inhomogeneities, the method of Section 1 is inapplicable to the problem of reconstructing the medium. The method presented here is a procedure for determining such variations. This method would be appropriate to the detection of velocity gradients in the seabed as well as to the general problems of subsurface mapping or geophysical exploration. Mathematically, the inverse problem considered here is to determine coefficients in a system of equations governing a wave propagation problem. It is assumed that the reference values of these coefficients (often constants) are available and that *variations from these reference values* are to be determined from observations of the field arising from known input sources. Physically, the coefficients to be determined, usually characterize the medium velocities or the acoustic impedance or some similar quantity.

For clarity of exposition, the discussion here will be restricted to media in which propagation is governed by the three-dimensional wave equation. In reference [16] by the authors, the inverse problem for electromagnetic waves and elastic waves is discussed, as well.

An essential feature of the inverse method presented here is that an integral equation is derived for a function which characterizes the velocity or impedance variation. This equation

is a Fredholm integral equation of the first kind; it has parameters in it which characterize the source and receiver locations. In a number of cases of source-receiver configurations of practical interest, this integral equation is invertible. Thus, a velocity or impedance profile (depth section) is obtained by direct processing of the observed data (time section) itself; i.e., by performing weighted quadratures on the data. This direct inversion of time section to depth section involves only one theoretical assumption: The subsurface variation must be "small." Even this limitation is not overly restrictive as can be seen from one of the examples below in which a 20% velocity variation was successfully migrated. In fact, the real world data restrictions--noise, attenuation, discretization and finiteness of observations, etc.,--are usually of greater concern than this theoretical linearization assumption.

2.1 An Integral Equation for Three-Dimensional Velocity Variation

It is assumed here that three-dimensional wave propagation is governed by the equation

$$(2.1) \qquad [\nabla^2 - v^{-2}(\underline{x}, z)\partial_t^2] \quad U(\underline{x}, z, t) = 0; \quad \underline{x} = (x,y).$$

Waves propagate in the semi-infinite medium, $z > 0$, measured *downward*. The operator ∂_t denotes a partial derivative with respect to time. It is the coefficient $v(\underline{x}, z)$ which is to be determined from probes and observations made at the upper surface, $z = 0$. For many cases of interest, the surface $z = 0$ separates two media of greatly differing impedances (e.g., air-water, air-earth). Hence, an appropriate boundary condition for (2.1) which introduces the probes is

$$(2.2) \qquad \partial_z U = \Phi(t, \underline{x}; \underline{\lambda}), \quad z = 0, \ \underline{\lambda} = (\lambda,\mu) \ .$$

The sources Φ characterized by the vector $\underline{\lambda}$ may be many types (See [16] for a discussion of plane wave sources). For definiteness, here, the discussion will be restricted to impulsive point sources located at $\underline{x} = \underline{\lambda}$, $z = 0$. Thus, the boundary condition actually treated is

$$(2.3) \qquad \partial_z U = -\delta(t)\ \delta(\underline{x} - \underline{\lambda}), \quad z = 0 \ .$$

To complete the specification of the direct problem for U, it is assumed that

$$U \equiv 0, \quad t < 0. \tag{2.4}$$

The reference value of the velocity, which is assumed known, will be denoted by $c(\underline{x}, z)$. Then, the variation, denoted by $\alpha(\underline{x}, z)$ is defined by the equation

$$v^{-2}(\underline{x}, z) = c^{-2}(\underline{x}, z)[\, 1 + \alpha(\underline{x}, z)] \,. \tag{2.5}$$

It is the variation α which is to be determined by means of observations of U made at surface points $\underline{x} = \underline{\xi}$, $z = 0$.

The total field U is decomposed into a primary field U_I, which is the solution in the absence of the variation α, and a scattered field U_S, which is the response to α. Thus

$$U(t, \underline{x}, z; \underline{\lambda}) = U_I(t, \underline{x}, z; \underline{\lambda}) + U_S(t, \underline{x}, z; \underline{\lambda}), \tag{2.6}$$

where U_I satisfies the following:

$$[\nabla^2 - c^{-2}\partial_t^2]\, U_I = 0, \quad z > 0; \tag{2.7}$$

$$\partial_z U_I = -\delta(t)\, \delta(\underline{x} - \underline{\lambda}), \quad z = 0; \tag{2.8}$$

$$U_I \equiv 0, \quad t < 0. \tag{2.9}$$

The argument $\underline{\lambda}$ is introduced into U, U_I, and U_S to emphasize their dependence on the source location. It then follows from the problems for U and U_I that U_S satisfies the following:

$$(2.10) \qquad [\nabla^2 - c^{-2}\partial_t{}^2]\, U_S = -\alpha\, c^{-2}\partial_t{}^2\, U;$$

$$(2.11) \qquad \partial_z U_S = 0, \quad z = 0;$$

$$(2.12) \qquad U_S \equiv 0, \quad t < 0.$$

An adjoint function V is now introduced, satisfying the following:

$$(2.13) \qquad (\nabla^2 - c^{-2}\partial_t{}^2)\, V = 0, \; z > 0;$$

$$(2.14) \qquad \partial_z V = -(\tau - t)\, H(\tau - t)\, \delta(\underline{x} - \underline{\xi}), \; z = 0; \; \underline{\xi} = (\xi, \eta);$$

$$(2.15) \qquad V \equiv 0, \; t > \tau.$$

It will be seen below that $\underline{\xi}$, τ denote the locations and times of observations at the upper surface. Furthermore, by comparing the problems for U_I and V, it can be seen that

$$(2.16) \qquad \partial_t{}^2\, V(t, \underline{x}, z; \underline{\xi}) = U(\tau - t, \underline{\xi}, z; \underline{x}).$$

Upon applying Green's theorem (in space and time) to the quantity,

$$U_S(\nabla^2 - c^{-2}\partial_t{}^2)V - V(\nabla^2 - c^{-2}\partial_t{}^2)\, U_S,$$

the following integral equation is obtained:

$$(2.17)\quad \int_0^\infty dz \int_{-\infty}^{\infty} dxdy\ \alpha(\underline{x}, z)\, c^{-2}(\underline{x}, z) \int_0^\tau dt\ U(t, \underline{x}, z; \underline{\lambda}) U_I(\tau - t, \underline{\xi}, z; \underline{x})$$

$$= \int_0^\tau dt U_S(t, \underline{\xi}, 0; \underline{\lambda})(\tau - t).$$

The right side here is a function of the field observations at the upper surface and, hence, known. The left side has two unknowns, namely, α and U_S. (A nonlinear system for these two unknowns is supplied by (2.17) and (2.10, 2.12).) However, U_S appears only in U and, therefore, only through the product αU_S. However, from (2.10) it is seen that U_S is itself of the order of α. Thus, for α small, it is expected that α U can be reasonably approximated by $\alpha\, U_I$. In this case, (2.17) becomes an integral equation for α alone, namely,

$$(2.18)\qquad \int_0^\infty dz \int_{-\infty}^{\infty} dxdy\ \alpha(\underline{x}, z)c^{-2}(\underline{x}, z)\int_0^\tau dt\ U_I(t, \underline{x}, z; \underline{\lambda})U_I(\tau\text{-}t, \underline{\xi}, z; \underline{x})$$

$$= \int_0^\tau dt\ U_S(t, \underline{\xi}, 0; \underline{\lambda})(\tau - t).$$

This is the basic linear integral equation for $\alpha(\underline{x}, z)$.

2.2 Direct Inversion for Backscatter Over a Medium with Two-Dimensional Velocity Variation

The integral equation (2.18) will now be specialized as follows. The reference velocity c will be taken to be a constant, so that U_I, defined by (2.7 - 9) is given by

$$(2.19) \qquad U_I(t, \underline{x}, z; \underline{\lambda}) = \delta(t - |\underline{x} - \underline{\lambda}|/c)/(2\pi|\underline{x} - \underline{\lambda}|).$$

The variation in α will be assumed to be independent of y, so that $\alpha(\underline{x}, z)$ will be replaced by $\alpha(x, z)$. In this case, both the sources and receivers will be restricted to the x axis. Finally, only backscattered (or CDP stacked) observations will be made, so that

$$(2.20) \qquad \underline{\lambda} = \underline{\xi} = (\xi, 0).$$

For this case, it is possible to carry out the y and t integrations in (2.18) to obtain

$$(2.21) \qquad \int_0^\infty dz \int_{-\infty}^{\infty} dx\, \alpha(x,z) H(c\tau/2 - \rho)\, [(c\tau/2)^2 - \rho^2]^{-\frac{1}{2}}$$

$$= -2\tau(\pi c)^2 \int_0^\tau dt\, U_S(t, \underline{\xi}, z; \underline{\xi})(\tau - t).$$

Here,

(2.22) $$\rho = [\,(x - \xi)^2 + z^2]^{\frac{1}{2}} \quad .$$

This integral equation can be solved by transform techniques. The result is

(2.23) $$\alpha(x, z) = 2ic^3\pi^{-1} \int_{-\infty}^{\infty} d\xi \int_{-\infty}^{\infty} dk_1 \int_{-\infty}^{\infty} dk_3 \int_{0}^{\infty} d\tau \int_{0}^{\tau} dt \Big\{ k_3(\tau^2 - \tau t)$$

$$\cdot U_S(t, \underline{\xi}, z; \underline{\xi}) \exp\{2ik_1(x-\xi) - 2ik_3 z + i\omega\tau\}\Big\};$$

$$\omega = c[\mathrm{sgn}\, k_3]\,(k_1^2 + k_3^2)^{\frac{1}{2}}$$

This is the direct inversion formula for the prescribed source receiver configuration for this section.

In [18], by the authors, this result was implemented for high frequency data synthetically produced for a number of layered models. Because of the high frequency bandlimiting, the data was processed for $\partial\alpha / \partial z = \alpha'$ rather than for $\alpha(x, z)$, itself. This merely requires multiplication of the integrand in (2.23) by $-2ik_3$. In accordance with the results of Section 1.3, not only the *location* of discontinuities may be determined but the *magnitude* of the discontinuities may be determined, as well. This *direct inversion* procedure produces a mapping of the interfaces and an estimate of the velocity variations across them.

The model used embodies other real world restrictions band limiting, namely;

(i) the observations are made only at *discrete* points on the line;

(ii) the observations are made only over a *finite* length of the line.

In these examples, the spacing between ξ points is 100 feet, the maximum array length is 8,000 feet and the bandwidth is 6 to 24 Hertz.

Synthetic data was generated for tilted planes at angles up to 75^{o}. Direct inversion reproduced these planes with three-place accuracy both in tilt angle and velocity variation.

In an earlier paper by the authors [19], a direct inversion formula was presented for the parabolic approximation to the wave equation used by CLAERBOUT [17] for 15^{o} wave equation migration. Synthetic data for tilted planes is used and the direct inversion is carried out analytically. The results show an error in tilt angle and in velocity estimation on the order of the fourth power of the angle of inclination. Numerical tests confirm this result, as well. This kind of error is already known to users of 15^{o} wave equation migration. The error is due to the underlying parabolic approximation and not a flaw of the direct inversion procedure or the wave equation migration procedure. Since the computational requirements of direct inversion for the wave equation are no more difficult than those for the parabolic approximation, the former is preferred to the latter by the authors.

Figure 8 shows a subsurface configuration for which synthetic data was graciously provided to us by the research group at Marathon Oil. The time section provided by them is depicted in Figure 9; Figure 10 is the result of our direct inversion procedure and Figure 11 shows our estimate from the output of various relevant quantities in the model. The lower two sets of numbers exhibit errors of less than 4%, while above the level, the errors are less than 1%.

The program was implemented on a time-sharing system on a Burroughs 6700 at the University of Denver. Output data was generated at a rate of 5 miliseconds per record. The number of records is defined as the product of

> (No. of geophones) x (No. of subsurface output points) x (Average number of non-zero time samples/trace).

Modifications of the original program have now improved *that rate to 2.4 miliseconds per record.*

2.3 Direct Inversion for Backscatter Over a Medium with Three-Dimensional Velocity Variation

When a three-dimensional velocity variation is to be detected, a two-dimensional source receiver array on the upper surface is required. When the reference speed is constant, U_I is again given by (2.19) but now $\underline{\lambda}$ is no longer restricted to the x axis. Now (2.18) becomes

$$(2.24) \qquad \int_0^\infty dz \int_{-\infty}^{\infty} dxdy \;\; \alpha(\underline{x}, z)\, \delta(\tau - 2\rho/c)\, /\rho^2$$

$$= -2(\pi c)^2 \int_0^T dt\; U_S(t, \underline{\xi}, 0; \underline{\xi})(\tau - t).$$

Here,

$$(2.25) \qquad \rho = [\,(x - \xi)^2 + (y - \eta)^2 + z^2\,]^{\frac{1}{2}} \quad .$$

The integral equation can again be inverted by integral transform methods. The result is

$$(2.26)\qquad \alpha(\underline{x}, z) = 2ic^3\pi^{-2} \int_{-\infty}^{\infty} d\xi d\eta \int_{-\infty}^{\infty} dk_1 dk_2 \int_0^{\infty} dk_3 \int_0^{\infty} d\tau \int_0^{\tau} dt \Big\{ k_3(\tau^2 - \tau t)$$

$$\cdot U_S(t, \underline{\xi}, z; \underline{\xi}) \exp\{2i[k_1(x-\xi) + k_2(y-\eta) - k_3 z] + i\omega\tau\}\Big\};$$

$$\omega = c[\mathrm{sgn}\, k_3]\,(k_1^2 + k_2^2 + k_3^2)^{\frac{1}{2}} \quad .$$

A computer program could be developed to implement this formula much as was described in the previous section. Output data would be generated at the same rate per record discussed at the end of the section. However, the number of records increases by a factor (say, N) for the new dimension in the geophone array and by a factor (say, N) for the output array. Thus, the computer time would increase by a factor of N^2. Thus, for the present, only analytical verifications have been carried out.

2.4 Direct Inversion for a Case with Separated Source and Receiver

Here it is assumed that $\alpha = \alpha(z)$, i.e., that α varies with z alone. Intuitively then, one would expect that only one experiment would be necessary to determine α. Again, it is assumed that c is constant so that U_I is given by (2.19). In this case, $\underline{\lambda}$ and $\underline{\xi}$ are taken to be fixed with

$$\underline{\xi} = -\underline{\lambda} . \tag{2.27}$$

In (2.18), the x, y and t integrations can all be performed yielding an elementary integral equation which can readily be inverted to yield

$$\alpha(z) = -4\pi c \int_0^{2(\lambda^2 + z^2)^{1/2}/c} dt \left[\frac{2}{c} \cdot \frac{\lambda^2 + 2z^2}{(\lambda^2+z^2)^{1/2}} - t \right] U_S(t, \underline{\lambda}, 0; -\underline{\lambda}). \tag{2.28}$$

For backscatter, it is only necessary to set $\underline{\lambda} = \underline{0}$ here to obtain the result

$$\alpha(z) = -4\pi c \int_0^{2z/c} dt \, [4z/c - t] \; U_S(t, \underline{0}, 0; \underline{0}). \tag{2.29}$$

2.5 Direct Inversion for a One-Dimensional Problem

In one dimension, one can generate synthetic wide band data by straightforward and economic means. This was done by GRAY [20] as a prelude to the analysis of strongly depth dependent velocities in three dimensions. An example of the output of this analysis is shown in Figure 12. The solid line is the assumed α (z) while the dots are the result of direct inversion on synthetically generated wide band backscattered data.

In [16], the authors also treated a case in which c(x) was not constant. The function u_I, the time transform of U_I, was expressible as a sum of exponentials and the integral equation was still invertible in closed form.

2.6 Direct Inversion In Free Space

Often in oceanographic and seismic exploration, the source is placed below the surface $z = 0$. In this case, the basic problem (2.1, 3,4) should be replaced by a *source* problem, with the delta function moved from the right side of (2.3) to the right side of (2.1) and the boundary condition (2.3) imposed on a new interface *above* $z = 0$, say at $z = z_0 < 0$.

If the effects of the reflections from the interface at z_0 can be accounted for (by no means an easy task), then such an experiment can be modeled by a free space problem in which the medium is "known" for $z < 0$ and assumed to vary only for $z > 0$. In this case, one still obtains (2.18) as the basic integral equation, but with U_I now a solution of the corresponding source problem in free space. For c = constant, the effect of this modification on U_I is to replace the factor of 2 on the right side of (2.19) by a 4. Since two factors of U_I appear in the kernel of the integral equation (2.18), the results (2.23, 26, 28) need only be modified by the introduction of a multiplier of 4 on the right side.

3. Non-Uniqueness in the Inverse Source Problem

In the previous sections the presentation assumes that the probing signal is an impulsive point source (See 1.1, 2.3). In practice, this is never the case. Thus, one is faced with the problem of "stripping away" source effects, i.e., performing source deconvolution, before proceeding to the inversion problem at hand.

In other problems, the source itself is the ultimate goal of the inversion process. This would be the case either for detection problems or for source synthesis problems (such as antenna design problems) in which the objective is to create a source to produce a given radiated field.

The objective of this section is to address the inverse source problem. The presentation follows the lines of [21] by the authors. It will be shown that there is a great deal of non-uniqueness in this problem. That is, a source cannot be completely reconstructed from observations of the field it radiates. The reason is that, in general, a certain part of the source simply does not radiate and, hence yields no clue, in the radiated field, to its presence. Thus, the solution to the inverse source problem is non-unique. Analytic characterizations of this non-uniqueness will be stated.

For source deconvolution, the non-uniqueness is not as serious a problem as it might at first appear to be. The reason is, that only the radiating part of the source is of interest in these

problems. This is so because only the radiating part of the source can effect the scattering obstacle or medium.

3.1 Analysis of the Direct Problem for Acoustic Waves

It is assumed that $U(\underline{x}, t)$ is a solution of the following problem in free space:

$$(3.1) \qquad [\nabla^2 - c^{-2}\partial_t{}^2]\, U(\underline{x}, t) = -F(\underline{x}, t);$$

$$(3.2) \qquad U \equiv 0, \quad F \equiv 0, \quad t < t_0 .$$

The source F is assumed to be confined to some sphere $x \leq a$, to be denoted by D. This region is itself confined to the interior of some larger region D_0. Observations of the radiated field will be made on ∂D, the boundary of D.

The Fourier time transform and space-time transforms are defined by the following:

$$(3.3) \qquad u(\underline{x}, \omega) = \int_{-\infty}^{\infty} dt\, U(\underline{x}, t) \exp\{i\omega t\} \;;$$

$$(3.4) \qquad \tilde{u}(\underline{k}, \omega) = \int_{-\infty}^{\infty} dt \int_{-\infty}^{\infty} dV\, U(\underline{x}, t) \exp\{-i\underline{k} \cdot \underline{x} + i\omega t\}$$

$$= \int_{-\infty}^{\infty} dV\, u(\underline{x}, \omega) \exp\{-i\underline{k} \cdot \underline{x}\} .$$

The time reduced problem equivalent to (3.1, 2) is

$$(3.5) \qquad (\nabla^2 + \omega^2/c^2)\, u(\underline{x}, \omega) = -f(\underline{x}, \omega)$$

with u outgoing,

$$(3.6) \qquad u(\underline{x}, \omega) \sim u_0(\hat{x}, \omega) \exp\{ i\omega x/c\} /(4\pi x),\ x \to \infty .$$

The solution to this problem can be expressed as a convolution of the source with the free space Green's function:

$$(3.7) \qquad u(\underline{x}, \omega) = \int_{x \leq a} dV'\, f(\underline{x}', \omega)\, g(r, \omega).$$

Here, dV' is the differential volume element in the prime variables,

$$(3.8) \qquad r = |\underline{x} - \underline{x}'| .$$

and

$$(3.9) \qquad g(r, \omega) = \exp\{i\omega r/c\} /(4\pi r).$$

The solution on ∂D is of interest. The origin of the coordinate system is taken to be in D. Then for $\underline{x}$ on ∂D, $x > a$. In this case, using the spherical harmonic expansion for g

(JACKSON, [22], p. 742), the solution u may be expressed as follows:

$$(3.10)\qquad u(\underline{x}, \omega) = i\omega c^{-1} \sum_{m=0}^{\infty} \sum_{n=-m}^{m} c_{mn}\, h_m^{(1)}(\omega x/c) Y_{mn}(\theta,\phi),\ x > a.$$

Here,

$$(3.11)\qquad c_{mn} = \int_0^a f_{mn}(x', \omega)\, j_m(\omega x'/c)\, x'^2 dx',$$

j_m and $h_m^{(1)}$ are the spherical Bessel function and Hankel function of the first kind, respectively, and Y_{mn} is the spherical harmonic of order mn. The functions f_{mn} are defined by

$$(3.12)\qquad f_{mn}(x, \omega) = \int_0^{\pi} \sin\theta\, d\theta \int_0^{2\pi} d\phi\, f(\underline{x}, \omega) Y_{mn}^*(\theta,\phi).$$

These functions are the coefficients of f in its spherical harmonic expansion

$$(3.13)\qquad f(\underline{x}, \omega) = \sum_{m=0}^{\infty} \sum_{n=-m}^{m} f_{mn}(x, \omega) Y_{mn}(\theta,\phi).$$

Since the spherical harmonics are a complete set of functions, knowledge of the coefficients f_{mn} constitutes knowledge of f itself. However, from (3.10, 11) it is seen that the radiated

field (i.e., u for $x > a$) is a function, not of the f_{mn}'s, but only of their *projections* on the Bessel functions j_m. Stated another way, the radiated field depends only on the projections of the source on the "doubly" infinite set of functions $\{j_m(\omega r/c)Y_{mn}(\theta,\phi)\}$. Since this class of functions is known not to be complete, knowledge of these projections does not suffice to determine f uniquely.

To demonstrate this non-uniqueness, one need only produce a non-zero function f for which all of the projections c_{mn} in (3.11) are zero. Such an example is provided by the function

$$(3.14) \qquad f(\underline{x}, \omega) = \begin{cases} \delta(\underline{x}) - j_0(\omega x/c)\left[4\pi \int_0^a j_0^{\,2}(\omega x/c)x^2\, dx\right]^{-1}, & x \leq a \\ 0, & x > a \end{cases}.$$

In this example, all of the functions f_{mn}, $m > 0$, are zero, while f_{00} is not. However, the projection of f_{00} on j_0 is zero. Thus for (3.10), the radiated field is zero, while the source is not. The inverse time transform in (3.14) produces a source in space-time confined spatially to the region $r \leq a$ and temporally to the interval $-a/c < t < a/c$.

An alternative characterization of this non-uniqueness can be deduced as follows. One solves the space time transformed problem for $\tilde{u}$ and inverts the time transform to obtain the representation of the solution

$$(3.15)\qquad U(\underline{x},\, t) = \pi^{-3}c/16 \sum_{\pm} \pm \int_{-\infty}^{\infty} k^{-1} d^3k\, \tilde{f}(\underline{k},\, \pm ck) \exp\{i\underline{k} \cdot \underline{x} \mp ckt\}\ .$$

Thus, the solution is seen to depend upon $\tilde{f}(\underline{k},\, \omega)$ only on the two sheets of a hyper-cone where $k = |\omega|\ /c$. Thus, the source need only have Fourier transform equal to zero on this hyper-cone in order that the radiated field be zero.

As an example, the source (3.14) has Fourier transform

$$(3.16)\qquad \tilde{f}(\underline{k},\, \omega) = 1 - \int_0^a j_0(\omega x/c) j_0(kx/c)\, x^2 dx \Big/ \int_0^a j_0{}^2(\omega x/c) x^2 dx$$

which indeed vanishes when $\omega = \pm ck$, but is clearly not identically zero.

For the electromagnetic case with current source distribution $\underline{J}(\underline{x},\, t)$, there will be no radiated field if

$$(3.17)\qquad [I - \hat{k}\hat{k}]\, \tilde{\underline{j}}(\underline{k},\, \pm ck) = \underline{0}.$$

Here I is the identity operator and $\hat{k}\hat{k}$ is the dyadic operator that yields the radial part of $\tilde{\underline{j}}$ in $\underline{k}$-space. The operator in (3.17) therefore produces the *transverse* (as opposed to radial) part of $\tilde{\underline{j}}$. Thus, *any* $\tilde{\underline{j}}$ which is purely radial will produce a non-radiating field. In addition, there will be no radiated field if only the transverse part of $\tilde{\underline{j}}$ vanishes on the appropriate hyper-cone.

3.2 Far Field Analysis of the Direct Problem

In the far field, $x >> x'$, the Green's function in (3.7) can be expanded just as in Section 1 (see equation 1.8). Then one finds

$$(3.18) \qquad u_0(\hat{x}, \omega) = \int_{x \leq a} dV\, f(\underline{x}, \omega) \exp\{ -i\omega \hat{x} \cdot \underline{x}/c \}$$

$$= \tilde{f}(\omega \hat{x}/c, \omega).$$

Here u_0 is the phase and range normalized far field scattering amplitude defined by (3.6). Thus, observation of the far field at all frequencies and in all directions provides an asymptotic expression for that part of $\tilde{f}(\underline{k}, \omega)$ which produces the radiated field.

It should be noted here that (3.18) provides an asymptotic solution of the inverse source problem for $\tilde{f}$ on the appropriate hyper-cone.

3.3 The Inverse Source Problem

The objective here is to develop methods for obtaining information about a source distribution solely in terms of observations made on ∂D.

The function $v(\underline{x}, \omega)$ is introduced, denoting any solution of the homogeneous reduced wave equation in the domain D. Then Green's theorem is applied on the domain D to the quantity $v(\underline{x}, \omega)\,[\nabla^2 + \omega^2 c^{-2}]\,u(\underline{x}, \omega) - u(\underline{x}, \omega)\,[\nabla^2 + \omega^2 c^{-2}]\,v(\underline{x}, \omega)$. Here, u is a solution of (3.5). The result is

$$(3.19) \qquad \int_{x \leq a} v(\underline{x}, \omega)\, f(\underline{x}, \omega)\, dV = \int_{\partial D} \left\{ u \frac{\partial v}{\partial n} - v \frac{\partial u}{\partial n} \right\} dA.$$

For any choice of $v(\underline{x}, \omega)$ of the prescribed type, this is an integral equation for $f(\underline{x}, \omega)$. A particular choice suggested by the discussion of the previous sections is any function in the class

$$(3.20) \qquad \Psi_{mn} = j_{mn}(\omega x/c)\, Y_{mn}(\theta,\phi), \quad m = 1, 2 \qquad |n| \leq m$$

with $v = \Psi^*_{mn}$, (3.19) becomes,

$$(3.21) \qquad c_{mn} = \int_{\partial D} \left\{ u \frac{\partial \Psi^*_{mn}}{\partial n} - \Psi^*_{mn} \frac{\partial u}{\partial n} \right\} dA.$$

Here, the c_{mn}'s are defined by (3.11). The source

$$(3.22)\qquad f_1(\underline{x},\omega) = \begin{cases} \sum_{m=0}^{\infty} \sum_{n=-m}^{m} c_{mn}\,\psi_{mn} : x \le a \\ 0 : x > a \end{cases},$$

will produce the same radiated field as f itself.† Thus, $f_1(\underline{x},\omega)$ would serve as an equivalent source for the purpose of source deconvolution.

Another choice of $v(\underline{x},\omega)$ is the plane wave

$$(3.23)\qquad v(\underline{x},\omega,\hat{k}) = \exp\{i\,\underline{k}\cdot\underline{x}\}\ ,\ k = |\omega|/c.$$

Here $\hat{k}$ may range over any of the continuum of directions in three space. Now (3.19) becomes

$$(3.24)\qquad \hat{f}(\underline{k},\omega) = \int_{\partial D} i\underline{k}\ \hat{n}\cdot u - \frac{\partial u}{\partial n}\ \exp\{i\underline{k}\cdot\underline{x}\}\,dA,\ k = |\omega|/c.$$

This is the exact result for which (3.18) is the far field asymptotic expansion. It should be noted that the plane wave, in fact, contains *all* of the functions ψ_{mn}; from [22], p. 767,

$$(3.25)\qquad \exp\{i\underline{k}\cdot\underline{x}\} = 4\pi \sum_{m=0}^{\infty} \sum_{n=-m}^{\infty} i^m\,\psi_{mn}\,Y^*_{mn}(\theta',\phi').$$

Here (θ',ϕ') are the spherical polar angles of $\underline{k}$.

---

†If the source f or the radiated field u has a convergent expansion in spherical harmonics, then the convergence in (3.22) is assured.

3.4 Uniqueness in the Inverse Source Problem

It has been shown that the inverse source problem has nonunique solutions. The only way to obtain a unique solution is to provide additional information about the source. Here, examples of this type will be presented.

Example 1: The point source

Here, it is assumed *a priori* that

$$F(\underline{x}, t) = \delta(\underline{x})\, G(t) \tag{3.26}$$

and that the observed data is consistent with this assumption (i.e., angularly independent). Although the general theory will provide the solution in this case, it is certainly easier to simply observe that

$$u(\underline{x}, \omega) = g(\omega)\, \exp\{i\omega x/c\}/(4\pi x) \tag{3.27}$$

and determine g uniquely (hence, $F(\underline{x}, t)$ uniquely) from observations in one direction.

A more interesting example is the following:

Example 2: The implusive source

Here,

$$F(\underline{x}, t) = \delta(t)\, G(\underline{x}), \tag{3.28}$$

and

$$\tilde{f}(\underline{k}, \omega) = \tilde{g}(\underline{k}), \quad \underline{k} = |\omega|/c. \tag{3.29}$$

The function $\tilde{f}$ is determined from observations by (3.23), for all choices of the direction of $\underline{k}$. All values of k are determined from frequency information.† Thus the function $\tilde{g}(\underline{k})$ (and hence $G(\underline{x})$) is known. Because of the *a priori* knowledge (3.28) about $F(\underline{x}, t)$, this function is now determined uniquely.

This problem of making the source unique by additional constraint is not well understood at all. The authors believe that a better understanding of the relation of uniqueness to side constraints would have important application to source synthesis and antenna design.

---

†The problems of aperture limiting will not be addressed here.

REFERENCES

[1] Bojarski, N. N., Three Dimensional Electromagnetic Short Pulse Inverse Scattering, Syracuse University Research Corporation, Syracuse, New York, NTIS # AD-845 126(1967)

[2] Lewis, R. M., Physical Optics Inverse Diffraction, IEEE Transactions on Antennas and Propagation, AP-17,3,308-314(1969)

[3] Bojarski, N. N., Inverse Scattering, Company Report #N00019-73-C-0312/F, prepared for Naval Air Systems Command, AD-775 235/5(1974)

[4] Perry, W. L., On the Bojarski-Lewis Inverse Scattering Method, IEEE Transactions on Antennas and Propagation, AP-22,6,826-829(1974)

[5] Tabbara, W., "On an Inverse Scattering Method", IEEE Transactions on Antennas and Propagation, AP-21, 245-247 (1973)

[6] Tabbara, W., "On the Feasibility of an Inverse Scattering Method", IEEE Transactions on Antennas and Propagation, AP-23, 446-448(1975)

[7] Rosenbaum-Raz, S., "On Scatterer Reconstruction from Far-field Data", IEEE Transactions on Antennas and Propagation, AP-24, 66-70(1976)

[8] Bleistein, N., Direct Image Reconstruction of Anomalies in a Plane via Physical Optics Far Field Inverse Scattering, J. Acoustical Soc. Amer., 59,2, 1259-1264(1976)

[9] Bleistein, N., Physical Optics Far Field Inverse Scattering in the Time Domain, J. Acoustical Soc. Amer., 60,6, 1249-1255 (1976)

[10] Mager, R. D., and Bleistein, N., An Approach to the Limited Aperature Problem of Physical Optics Farfield Inverse Scattering, Denver Research Institute Report #MS-R-7704(1976)

[11] Baker, B. B., and Copson, E. T., Mathematical Theory of Huygens Principle, 2nd Ed., (Oxford, 1950)

[12] Bleistein, N. and Handelsman, R. A., Asymptotic Expansions of Integrals (Holt, Rinehart and Winston, Inc., New York, 1975)

REFERENCES
(Continued)

[13] Majda, A., High Frequency Asymptotics for the Scattering Matrix and the Inverse Problem of Acoustic Scattering, Comm. Pure Appl. Math., 30, 165-194(1977)

[14] Armstrong, J., An Analysis of the Aperture Limited Fourier Inversion of Characteristic Functions, Thesis, in preparation(1977)

[15] Bleistein, N. and Cohen, J. K., Application of a New Inverse Method to Non-Destructive Evaluation, Denver Research Institute Report #MS-R-7716(1977)

[16] Cohen, J. K. and Bleistein, N., An Inverse Method for Determining Small Variations in Propagation Speed, SIAM J. Appl. Math., 32,4, 784-799(1977)

[17] Claerbout, J., Fundamentals of Geophysical Data Processing (McGraw-Hill, New York, 1976)

[18] Cohen, J. K. and Bleistein, N., A Direct Inversion Procedure for Acoustic Waves, Denver Research Institute Report #MS-R-7803(1977)

[19] Bleistein, N. and Cohen, J. K., A Note on a Direct Inversion Procedure for Claerbout's Equations. Denver Research Institute Report #MS-7-7802(1977)

[20] Gray, S., Direct Inversion for Strongly Depth Dependent Velocity Profiles, Thesis, in preparation(1977)

[21] Bleistein, N. and Cohen, J. K., Non-uniqueness in the Inverse Source Problem in Acoustics and Electromagnetics, J. Math. Phys., 18,2, 194-201(1977)

[22] Jackson, J. D., Classical Electrodynamics, 2nd Ed. (Wiley, New York, 1975)

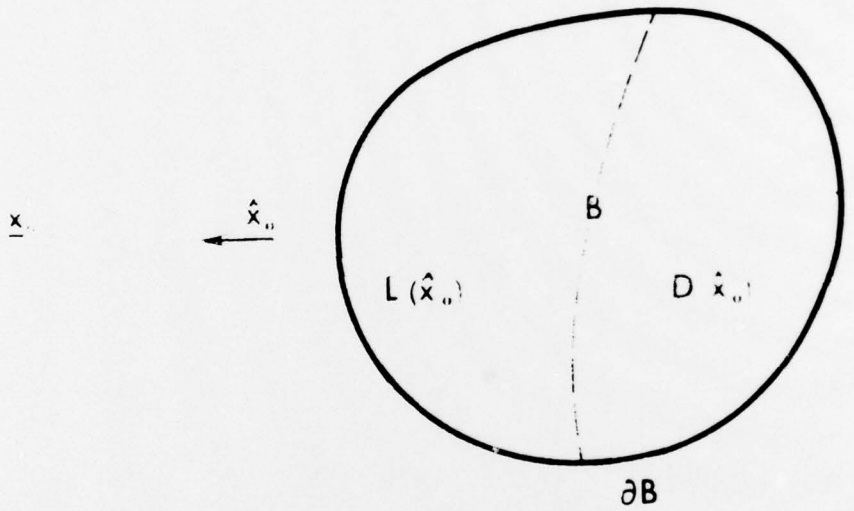

FIGURE 1

55

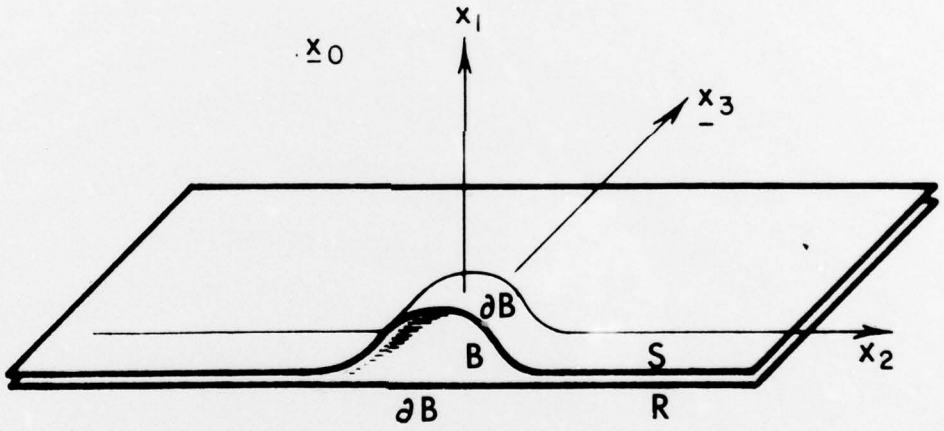

FIGURE 2

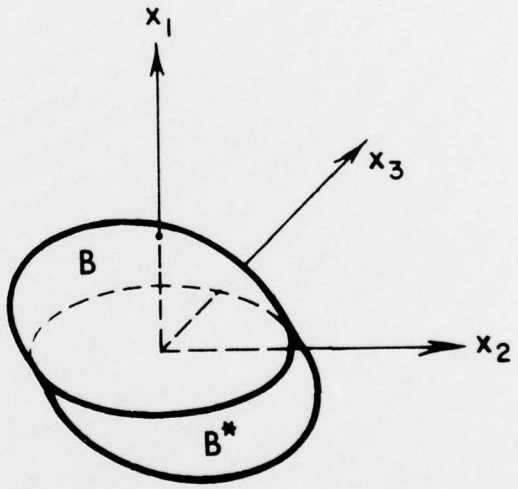

FIGURE 3

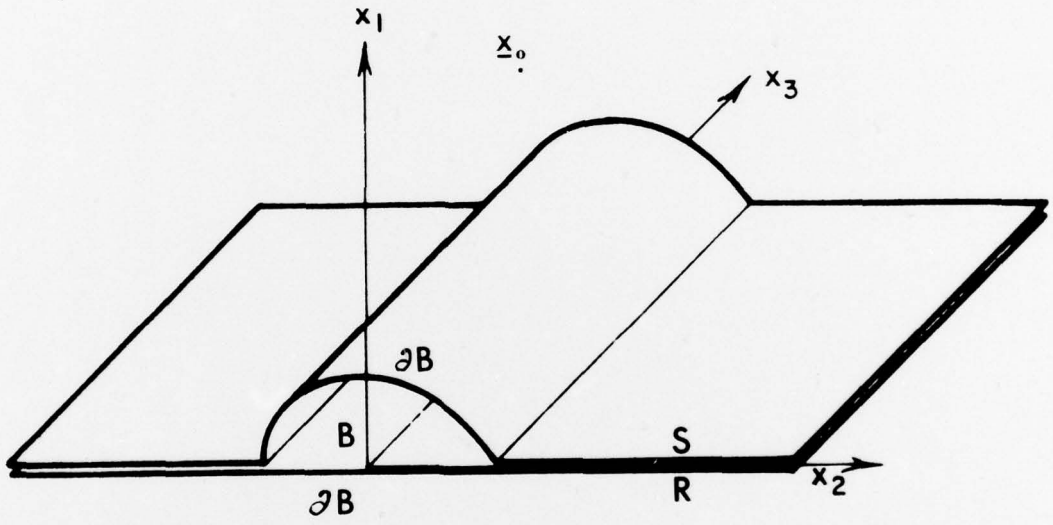

FIGURE 4

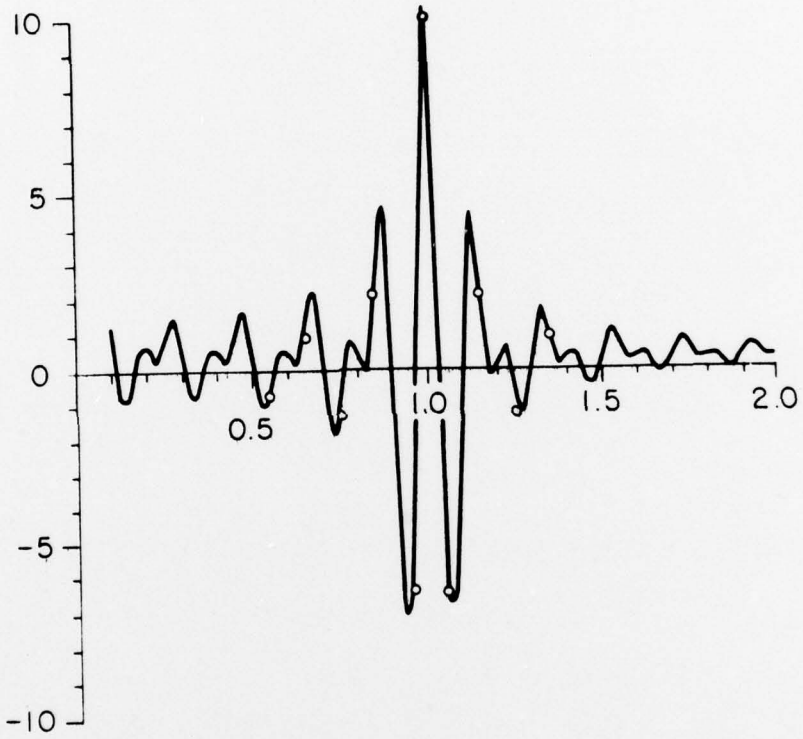

FIGURE 5

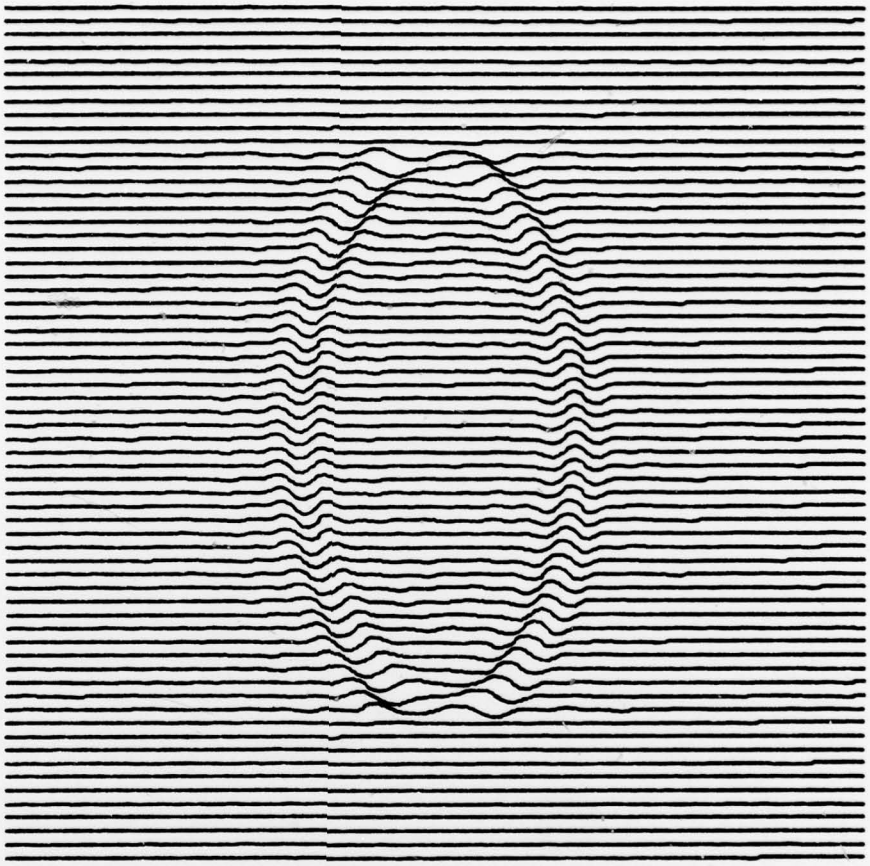

K Range 9-27

FIGURE 6

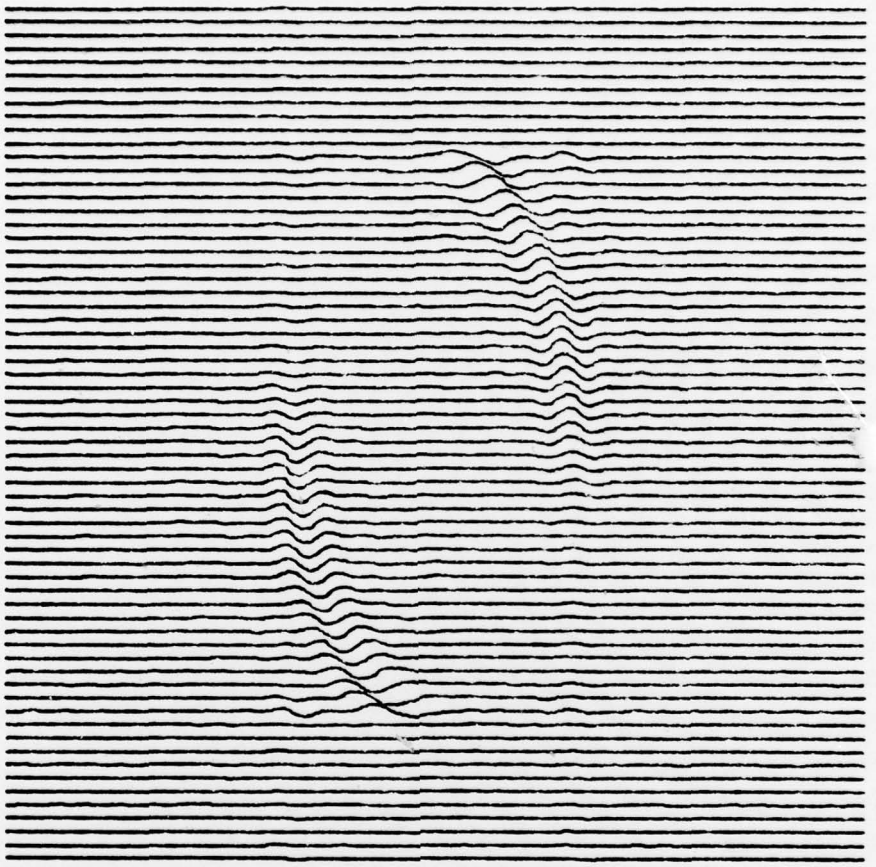

K Range 9 -27

Angular Range $\begin{matrix} 0°-90° \\ 180°-270° \end{matrix}$

FIGURE 7

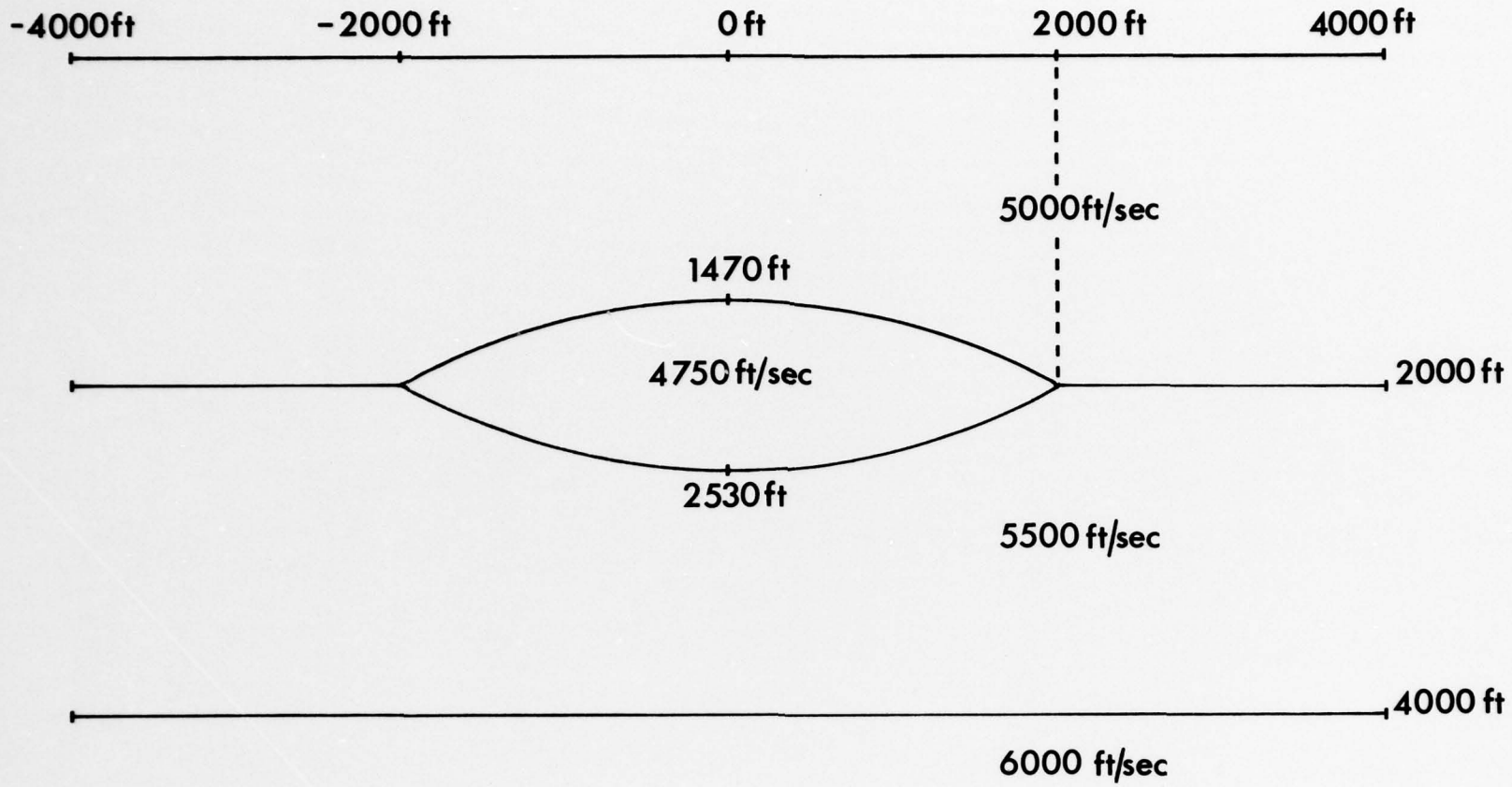

62

ACTUAL MODEL

FIGURE 8

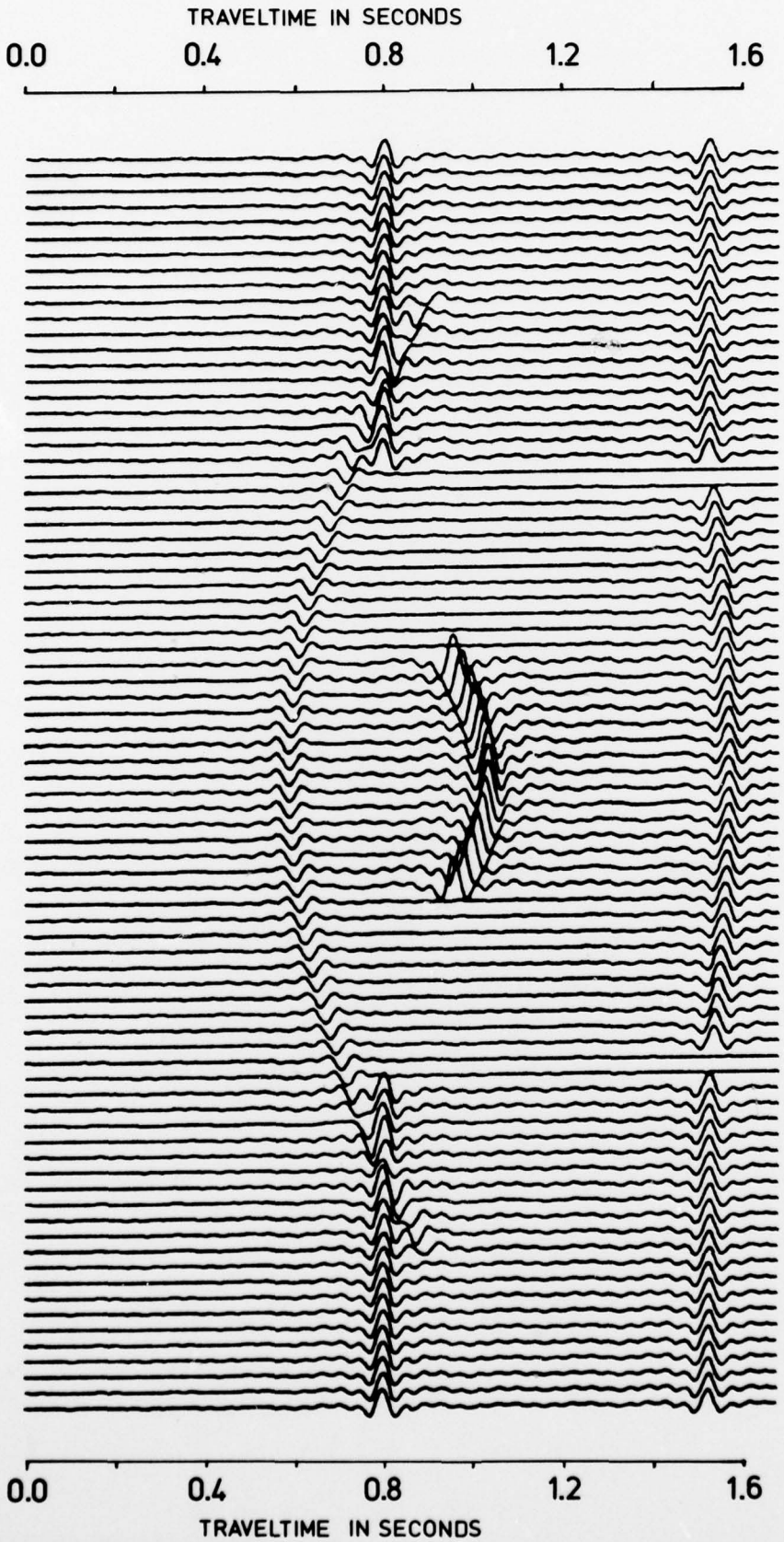
TRAVELTIME IN SECONDS
0.0
0.4
0.8
1.2
1.6
0.0
0.4
0.8
1.2
1.6
TRAVELTIME IN SECONDS

FIGURE 9

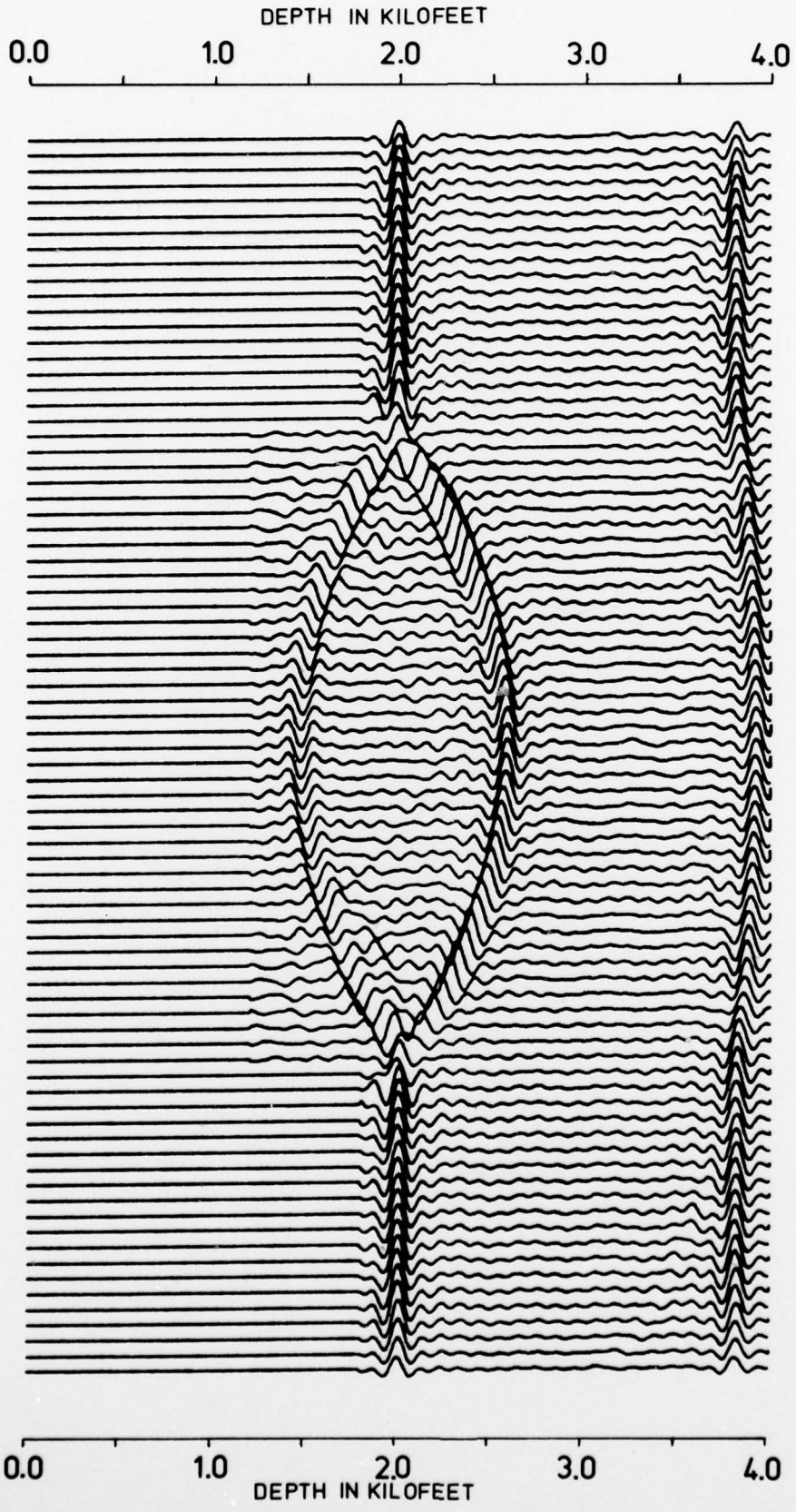
DEPTH IN KILOFEET
0.0
1.0
2.0
3.0
4.0
0.0
1.0
2.0
3.0
4.0
DEPTH IN KILOFEET

FIGURE 10

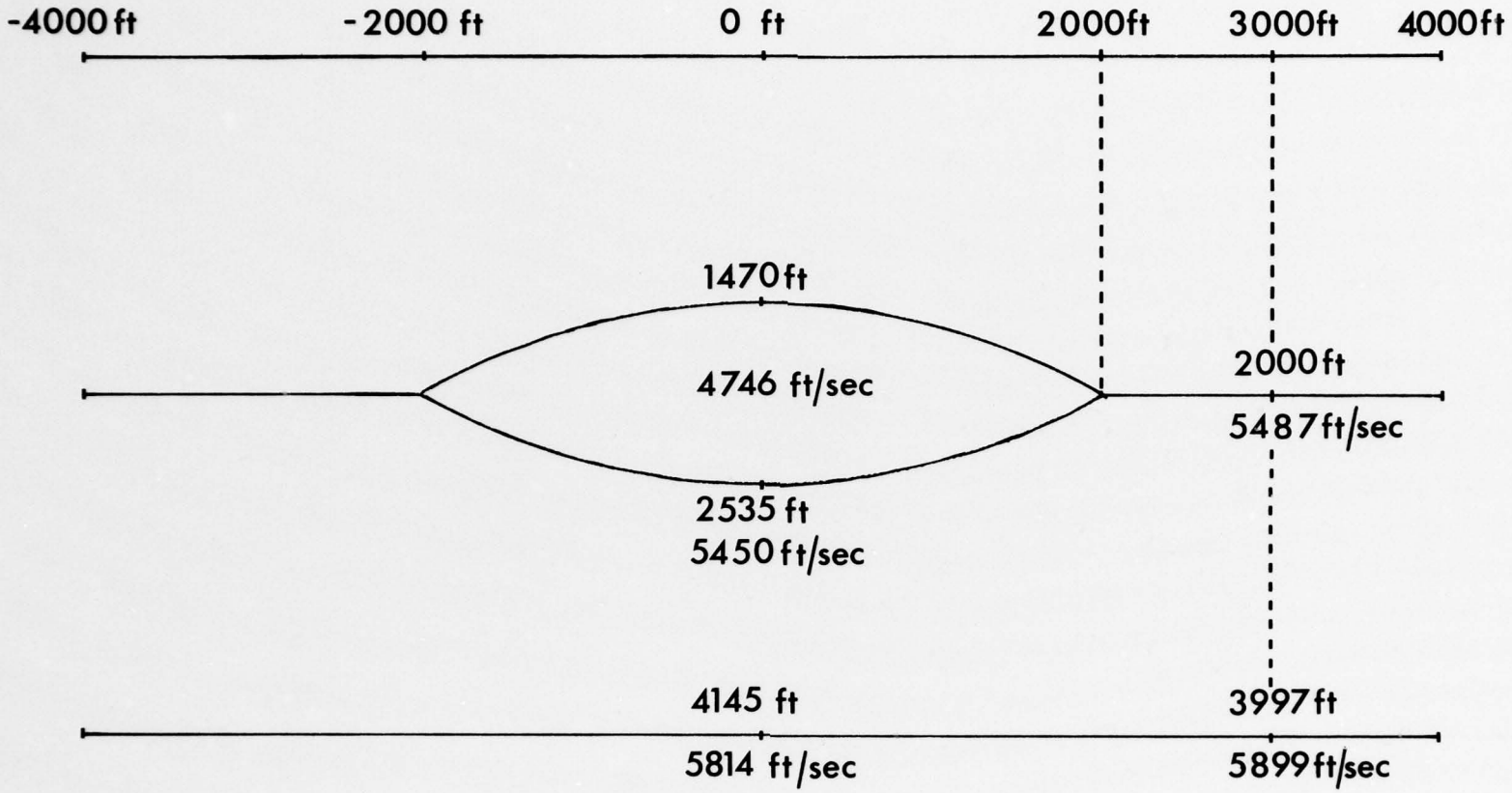

COMPUTED MODEL

FIGURE 11

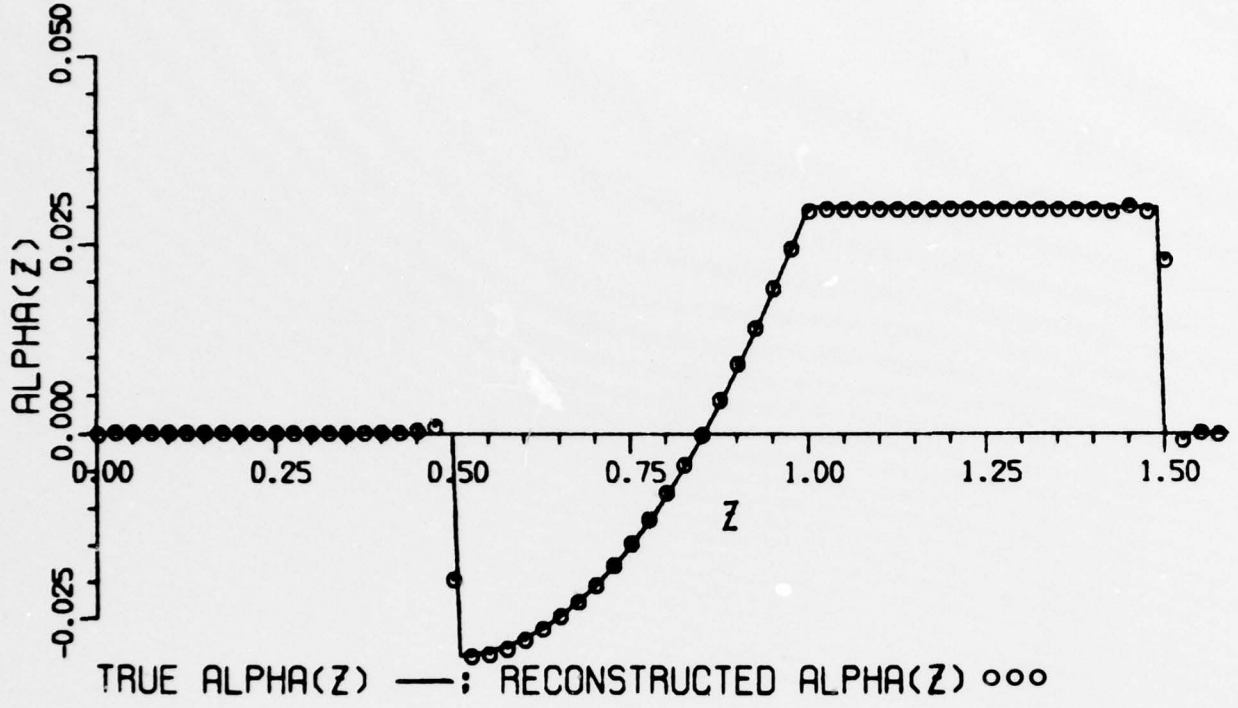
ALPHA(Z)
0.050
0.025
0.000
-0.025
0.00
0.25
0.50
0.75
1.00
1.25
1.50
Z
TRUE ALPHA(Z) ——; RECONSTRUCTED ALPHA(Z) ooo

FIGURE 12

UNCLASSIFIED

SECURITY CLASSIFICATION OF THIS PAGE (When Data Entered)

REPORT DOCUMENTATION PAGE	READ INSTRUCTIONS BEFORE COMPLETING FORM
1. REPORT NUMBER: MS-R-7806	2. GOVT ACCESSION NO.
3. RECIPIENT'S CATALOG NUMBER	
4. TITLE (and Subtitle): A Survey of Recent Progress on Inverse Problems	5. TYPE OF REPORT & PERIOD COVERED: Technical Rept.
6. PERFORMING ORG. REPORT NUMBER	
7. AUTHOR(s): Norman Bleistein and Jack K. Cohen	8. CONTRACT OR GRANT NUMBER(s): N00014-76-C-0079
9. PERFORMING ORGANIZATION NAME AND ADDRESS: Department of Mathematics, University of Denver, Denver, Colorado 80208	10. PROGRAM ELEMENT, PROJECT, TASK AREA & WORK UNIT NUMBERS: NR 041-434/6-10-75
11. CONTROLLING OFFICE NAME AND ADDRESS: Office of Naval Research, Arlington, Virginia 22217	12. REPORT DATE: December 1, 1977 (1 Dec 77)
	13. NUMBER OF PAGES: 67
14. MONITORING AGENCY NAME & ADDRESS (if different from Controlling Office)	15. SECURITY CLASS. (of this report): (12) 71 p.
	15a. DECLASSIFICATION/DOWNGRADING SCHEDULE

16. DISTRIBUTION STATEMENT (of this Report)

This document has been approved for public release and sale; its distribution is unlimited.

17. DISTRIBUTION STATEMENT (of the abstract entered in Block 20, if different from Report)

18. SUPPLEMENTARY NOTES

19. KEY WORDS (Continue on reverse side if necessary and identify by block number)

Inverse Source
Velocity Inversion
POFFIS identity
Acoustic Waves
Backscatter
Seismic exploration

20. ABSTRACT (Continue on reverse side if necessary and identify by block number)

Over the past few years, the authors have been engaged in a coordinated research program on inverse problems. By this time, the results have been spread over a number of different papers. This review provides an opportunity to collect those results, to filter some of the work that has proven to be of less interest and to incorporate into the presentation new insights that have been developed during this research project.

Cont. on next page

DD FORM 1 JAN 73 1473 EDITION OF 1 NOV 65 IS OBSOLETE
S/N 0102-014-6601

UNCLASSIFIED

SECURITY CLASSIFICATION OF THIS PAGE (When Data Entered)

406 854

This report describes the three main segments in the research program:

i) physical optics farfield inverse scattering (denoted by the alliteration POFFIS);

ii) seismic or subsurface profiling in media with small variations in propagation speed;

iii) analysis of the inverse source problem.